



The influence of gas composition on Pd-based catalyst activity in methane oxidation – inhibition and promotion by NO

Nadezda Sadokhina^a, Gudmund Smedler^b, Ulf Nylén^c, Marcus Olofsson^d, Louise Olsson^{a,*}

^a Chemical Engineering, Chalmers University of Technology, 412 96, Gothenburg, Sweden

^b Johnson Matthey AB, 421 31, Västra Frölunda, Sweden

^c Scania CV AB, 151 87 Södertälje, Sweden

^d AVL MTC Motortestcenter AB, Box 223, 13623, Haninge, Sweden



ARTICLE INFO

Article history:

Received 20 March 2016

Received in revised form 28 June 2016

Accepted 14 July 2016

Available online 15 July 2016

Keywords:

Methane oxidation

NO

H₂O

Inhibition

Promotion

ABSTRACT

The individual influence, as well as the combined effect of H₂O and NO on the activity of Pd/Al₂O₃, PtPd/Al₂O₃ and PtPd/CeAl₂O₃ catalysts in complete methane oxidation under lean conditions were investigated. Under temperature-programmed ramping experiments the activity was severely inhibited in the presence of 5 vol.% H₂O in the reaction mixture. We propose that this is due to blocking by both water and hydroxyl species. Under the influence of NO without water in the gas flow, it was found that the methane oxidation activity was partly suppressed, due to blocking of active sites. Indeed TPD performed after ramping experiments showed NO_x storage on the catalyst. Contrary to the negative effect of NO in the dry case, the promotional NO effect on the activity was observed when water was co-fed, comparing the case with only water presence. The promotional NO effect was confirmed with isothermal experiments, where e.g. the methane conversion decreased from initial 96% to 25% after 10 h of exposure in CH₄–O₂–H₂O mixture at 450 °C over the Pd/Al₂O₃ sample, while the decrease was only from 88% to 60% when catalyst was exposed to CH₄–O₂–H₂O–NO mixture. We propose that the reason is that the NO reacts with the hydroxyl species to form HNO₂, which reduces the water deactivation effect.

© 2016 Elsevier B.V. All rights reserved.

1. Introduction

Vehicles powered by lean burn natural and bio gas engines have received great attention due to several important benefits, in particular decreasing the raw emissions of nitrogen oxides and particulate matter compared to diesel and gasoline engines [1]. Methane is a major pollutant obtained from natural gas vehicles (NGVs) and can be oxidized to water and carbon dioxide on an oxidation catalyst placed in a catalytic converter. The design of a catalyst with a high level of activity at low temperatures and simultaneously high stability under an NGV exhaust gas remains an important issue. Palladium supported on γ -alumina is the most well-studied catalyst of the total methane oxidation in application to the NGV emission control [2,3] with the ability to activate a stable methane molecule. The active phase of the catalyst has been established to be PdO or Pd–PdO pairs at low temperature and Pd metallic at high temperature [4–9]. However, deactivation of the

catalyst occurs under an excess of oxygen in the presence of water vapor in the exhaust of NGVs. Although monometallic Pt-based catalysts are less active than monometallic Pd-based catalysts under lean conditions [10,11], several studies have reported that the stability and resistance of Pd-catalysts to poisons may be improved by adding Pt promoter [2,12,13]. One possible explanation may be that Pt inhibits the sintering of PdO particles leading to the longer catalyst life under wet lean reaction conditions [13–15]. However, it has been illustrated that the effects of Pt on catalytic activity are not straightforward [16]; Pt can act as either a promoter or an inhibitor of activity depending on the variety of factors including the extent of PdO formation, the strength of the support interactions, and the stabilization of metallic Pd, as well as noble metals loading. Moreover, the performance of the catalyst strongly depends on the nature of the support. For complete methane oxidation, alumina is a well-known support used for noble metal-based catalyst synthesis [2,3]. However, it has been demonstrated that the use of Ce-doped alumina instead of pure γ -Al₂O₃ results in increased mechanical properties of the support, stabilizing it against area loss [2,7,17–19]. However, the Ce promoting effect is dependent upon Ce loading

* Corresponding author.

E-mail address: louise.olsson@chalmers.se (L. Olsson).

[20]. It was shown that catalysts containing a high amount of Ce did not promote the methane oxidation.

There are several kinetic studies of catalytic CH_4 oxidation reported in the literature, mainly focusing on the investigation of monometallic Pd- or Pt-based catalysts [9,21–25]. However, there are fewer studies available that use bimetallic catalysts which attract large practical interest, since Pt promoters can improve stability of the catalyst under operating conditions with water in a gas flow, as well as can hinder the growth of Pd and PdO particle size [14,16,26]. The apparent activation energies reported for methane oxidation on PdO -supported catalysts were in a broad range from 60 to 190 kJ/mol depending on the water vapor presence in the gas feed [9,21,24,25,27]. Typical reaction orders reported in previous studies of methane oxidation were 0.6–1 for methane, 0 for oxygen, −1 for water, and 0 for CO_2 at low concentrations [25,27]. It should be noted that water inhibition was found to be significant at a temperature lower than 450 °C [28] and may be related to hydroxyl groups formed on Pd-particle surface or on the support [23,29]. Furthermore, NO was found to promote methane oxidation over palladium containing catalysts. Interestingly, Hurtado et al. [30] observed a slightly positive effect on methane conversion when adding 60 ppm NO_2 using a $\text{Pd}/\text{Al}_2\text{O}_3$ catalyst. Furthermore, Gremminger et al. [31] observed that they could reactivate the $\text{PtPd}/\text{Al}_2\text{O}_3$ catalyst after reaction conditions using a mixture of NO and NO_2 and presented the hypothesis that Pt and Pd particles are stabilized in different ways in the presence of NO_x , based on TEM results. However, there is limited knowledge about the interactions between NO and water during methane oxidation.

The specific objective of this paper is to study the influence of H_2O and NO on the methane oxidation and the effect of adding Pt and Ceria to the $\text{Pd}/\text{Al}_2\text{O}_3$ catalyst. Flow reactor experiments are combined with catalyst characterization using BET, TEM, XRD, TPO and TPR.

2. Experimental

2.1. Catalyst preparation and characterization

Powder samples with 3.8 wt.% of the total amount of noble metal were prepared using wet impregnation of commercial γ - Al_2O_3 (Sasol, Puralox SBa-200) and 20 wt.% Ce-doped Al_2O_3 (Sasol, Puralox SCFa-160/Ce20), both calcined at 900 °C for 2 h in the oven. Initially, a slurry of the support material was prepared, with a pH stabilized at 4 using a diluted HNO_3 solution. In addition, Pt- and Pd- precursor solutions were prepared by a dilution of $\text{Pt}(\text{NO}_3)_2$ (Heraeus GmbH, 15.12 wt.% Pt) and $\text{Pd}(\text{NO}_3)_2$ (Heraeus GmbH, 17.27 wt.% Pd) in milliQ water. The precursor solution was added dropwise to the support slurry and was stirred for 1 h at a pH of 2. After stirring, the solution was frozen with liquid nitrogen and dried under vacuum. The powder obtained was calcined at 500 °C for 2 h in the oven. The powder of the bimetallic catalysts were prepared by a sequence wet impregnation method, to obtain 0.6 wt.% Pt and 3.2 wt.% Pd.

The powder obtained was placed on ceramic monoliths ($D = 21$ mm, $L = 20$ mm; 400 cpsi) by means of the following procedure. A slurry of 20 wt.% dry content (catalyst powder and 'binder' (Sasol, Disperal P2) at a 4:1 ratio) was prepared by mixing the solid phase with a solution of ethanol and distilled water (ratio of pure ethanol to water was 1:1). The empty monoliths were calcined at 600 °C for 2 h prior to the washcoating. The monoliths were coated with the catalyst slurry by immersing the monolith into the slurry; blowing away the excess of slurry by air flow, drying at 100 °C for 2 min and calcining at 600 °C for 2 min using a hot gun. This procedure was repeated until the monoliths had been coated with the desired amount of washcoat (mass of washcoat = 500 ± 10 mg). The

monoliths covered by washcoat were then calcined at 600 °C for 2 h in the oven.

The BET surface area of fresh prepared samples and supports pretreated at high temperature was determined using a TriStar 3000 by measuring N_2 adsorption isotherms at the temperature of liquid N_2 . The X-ray diffraction (XRD) patterns were recorded using a D5000 powder Siemens Diffractometer. Prior to the measurements, the powder of the fresh synthesized catalysts was pretreated in a way similar to the pretreatment of the washcoated monoliths before the catalytic activity tests (Section 2.2 below). However, no water nor any CO was present during the pretreatment of the samples used in XRD measurements.

A transmission electron microscopy (TEM) analysis was performed to examine the particle size of the $\text{PtPd}/\text{CeAl}_2\text{O}_3$ catalysts, as well as testing if any alloys had been formed between Pt and Pd. After the catalytic activity tests, the powder of sample was collected from the monolith for TEM analysis. In addition, powder (pre-treated in the same way as for XRD) was used in the TEM measurements. The samples were pestled in an agate mortar and then placed on carbon films using TEM Cu grids. The particles were imaged using an FEI Titan 80–300 TEM with a probe Cs (spherical aberration) corrector operated at 300 kV. The images were recorded using a high angle annular dark field (HAADF) detector in the scanning TEM imaging mode (STEM), providing a Z number contrast. The electron probe size was about 0.2 nm for this study. The chemical characterization of particles was made by energy dispersive X-ray (EDX) spectroscopy.

2.2. Catalytic activity measurements

Catalytic activity tests were performed in a fixed-bed flow reactor. The monolith samples ($D = 21$ mm; $L = 20$ mm) were placed in a quartz tube with an inner diameter of 22 mm and a length of 80 cm, equipped with an insulated heating wire controlled by a Eurotherm temperature-controller. The temperature was measured by two thermocouples; one of them positioned in the center of the sample and the second one that 10 mm upstream of the monolith. The temperatures presented in this paper are derived from the thermocouple that had been placed in the middle of a monolith. The total gas flow was held constant at 3500 ml/min ($\text{GHSV} = 30,000 \text{ h}^{-1}$) and was controlled by a system of Bronkhorst mass flow controllers. Water was evaporated and dosed by CEM (controlled evaporator and mixer) system (Bronkhorst High-Tech B.V.). The outlet gas composition was monitored using an MKS MultiGas 2030 HS FTIR gas analyzer.

The procedure for activity tests of the samples was: (1) degreasing the catalyst, (2) pre-treatment of the catalyst, (3) activity test for an methane oxidation ramping from 150 to 700 °C (heating step) and back to 150 °C (cooling step) at a rate of 5 °C/min, (4) repeating the temperature ramp in step (3) and (5) temperature-programmed desorption (TPD) in Ar flow. The details of the above mentioned five steps are described as follows. Step 1: Reduction at 500 °C in 2 vol.% H_2 in Ar flow for 30 min followed by a treatment at 700 °C under lean conditions (0.05 vol.% CH_4 , 0.05 vol.% NO, 8 vol.% O_2 , 0.03 vol.% CO, 5 vol.% H_2O , Ar) for 60 min; then under rich conditions (2 vol.% H_2 , 5 vol.% H_2O , Ar) for 20 min and again under lean conditions for 60 min. Thereafter, the sample was purged with Ar for 10 min. Step 2: Pre-treatment at 700 °C using 8 vol.% O_2 , in Ar flow for 30 min; the sample was then cooled down in Ar flow to the set temperature. Steps 3 and 4: Activity tests during heating and cooling using 0.05 vol.% CH_4 , 8 vol.% O_2 , 0 or 0.05 vol.% NO, 0 or 5 vol.% H_2O , balanced by Ar. Step 5: TPD in Ar flow from 150 °C to 700 °C at a ramp rate of 20 °C/min in 1000 ml/min. The experiments without water and with water in a gas flow refer to as 'dry' and 'wet', respectively.

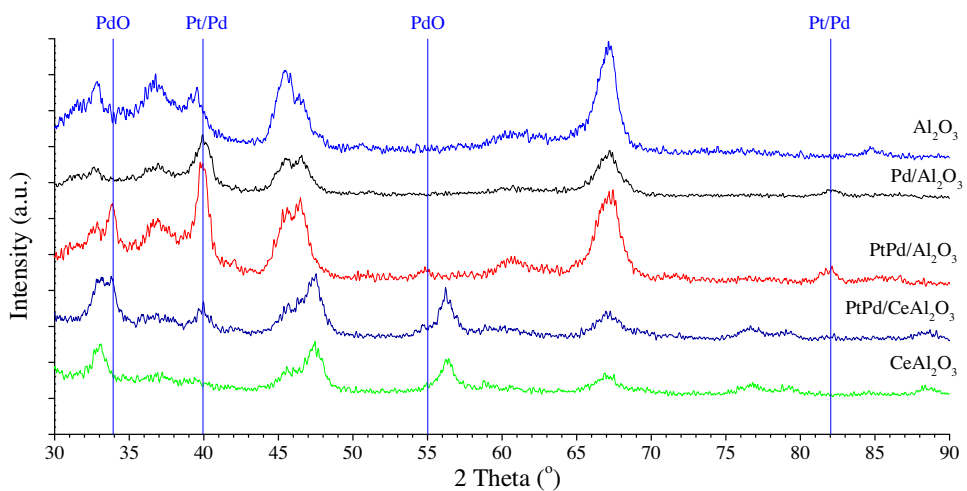


Fig. 1. XRD patterns of the powder samples pre-treated in a similar way as before catalytic activity tests and the supports pre-treated at 900 °C in air.

The same procedure (step 2–5) was used every time when the methane oxidation activity was tested under new gas composition. Step 1 (degreening) was only performed for the fresh catalyst.

2.3. Temperature-programmed oxidation (TPO) and reduction (TPR) experiments

TPO and TPR measurements of powder samples (circa 100 mg) were performed in a fixed-bed flow reactor with an internal diameter of 5 mm, coupled with a HPR-20 101 RC quadrupole mass spectrometer (Hiden Analytical). Mass spectrometer was operated in a standard residual gas analysis (RGA) mode where ions are created in an internal electron impact ionisation source, with the electron energy adjusted at 70 eV. In RGA mode positive ions are extracted for the monitoring. The signals with $m/z = 13, 44, 36, 28, 18$ and 2 were monitored to measure the concentrations of CH₄, CO₂, O₂, CO, H₂O and H₂, respectively.

The tests were carried out using a total gas flow of 20 ml/min. Prior to the first use, the sample had been pre-treated at 500 °C in 2 vol.% H₂ in Ar flow for 30 min. The temperature was thereafter increased up to 700 °C in Ar flow. At this temperature, the powder was treated under lean conditions (0.05 vol.% CH₄, 0.05 vol.% NO, 8 vol.% O₂, Ar) for 60 min twice with a treatment under rich conditions (2 vol.% H₂, Ar) for 20 min in between.

Before TPO experiments, the sample had been reduced using 2 vol.% H₂ in Ar at 500 °C during 30 min and cooled down to room temperature (RT) in Ar flow. TPO experiments were carried out in 0.5 vol.% O₂ in Ar flow with a linear temperature increase of 10 °/min from the RT up to 800 °C and then back down to 100 °C.

After TPO experiments, the sample was oxidized under 5 vol.% O₂ in Ar at 500 °C during 1 h and cooled down to RT using the same flow. TPR experiments were then carried out using 0.2 vol.% CH₄ in Ar flow with a linear temperature increase of 10 °/min from RT up to 800 °C. When the temperature reached 800 °C, the sample was exposed to 0.2 vol.% CH₄ in Ar flow for 30 min and the methane was then replaced by 0.5 vol.% O₂ at the same temperature for 30 min. This step was followed by a cooling-down period in Ar flow to room temperature.

3. Results and discussion

3.1. Characterization of the samples

The BET surface area of the samples and the support materials was measured and the results for the catalysts are shown in Table 1.

Table 1
Composition of the catalysts tested in methane oxidation.

Sample	Pt, wt.% (g/ft ³)	Pd, wt.% (g/ft ³)	Pt:Pd atomic ratio	Surface area, m ² /g
Pd/Al ₂ O ₃	0 (0)	3.8 (63)	0:1	133
PtPd/Al ₂ O ₃	0.6 (10.5)	3.2 (52.5)	1:10	134
PtPd/CeAl ₂ O ₃	0.6 (10.5)	3.2 (52.5)	1:10	120

The BET surface area of Al₂O₃ and CeAl₂O₃ decreased after the high temperature pre-treatment at 900 °C, from 200 to 132 m²/g and from 160 to 114 m²/g, respectively. Despite this pretreatment, the BET surface area of the resulting bimetallic PtPd/Al₂O₃ and PtPd/CeAl₂O₃ samples was high, 134 m²/g and 120 m²/g, respectively, although it was lower than the typical BET surface area of a fresh catalyst. A similar BET surface area (133 m²/g) was measured on the fresh monometallic Pd/Al₂O₃ catalyst.

In addition, the catalysts were characterized using X-ray diffraction (XRD) technique and the results are summarized in Fig. 1. XRD spectra of the 3 samples were compared with the XRD spectra of the supports pretreated at high temperature. In addition to the diffraction peaks of Al₂O₃ and 20 wt.% CeAl₂O₃, for both bimetallic catalysts, PdO reflections were visible at 2θ = 34°; however, only minor peaks were observed at 55° in the XRD spectra and the same was observed in literature [16,31]. No PdO reflections were detected for monometallic sample, suggesting palladium oxide particles are smaller in size than the particles obtained on bimetallic samples. For this sample, merely the reflection peaks of metallic Pd were detected. Additional peaks were observed at 2θ = 40° and 82° which are visible with varying intensity for all samples. At these 2θ the reflection of either metallic Pd or metallic Pt could be detected; it is difficult to distinguish between these peaks; they will be referred to as metal Pt/Pd particles. The peak of Pt/Pd reflection detected on PtPd/Al₂O₃ were sharper compared with peak observed on PtPd/CeAl₂O₃. Based on the data, we suggest that the bimetallic Ce-free sample contained large metal particles in contrast to the bimetallic Ce-containing sample where Pt/Pd particles are smaller in size or present in the oxide form.

Furthermore, powder of the 0.6Pt – 3.2Pd/CeAl₂O₃ sample tested in methane oxidation was scraped off the monolith and used for TEM and STEM analysis, which are depicted in Fig. 2 (Top). The STEM and TEM results show spherical particles with a size of approx. 10–20 nm. The reason for the formation of large particles is likely that the sintering occurred during the catalyst pre-treatment at 700 °C during alternation between lean and rich conditions. Additional factor for the large particle formation is that

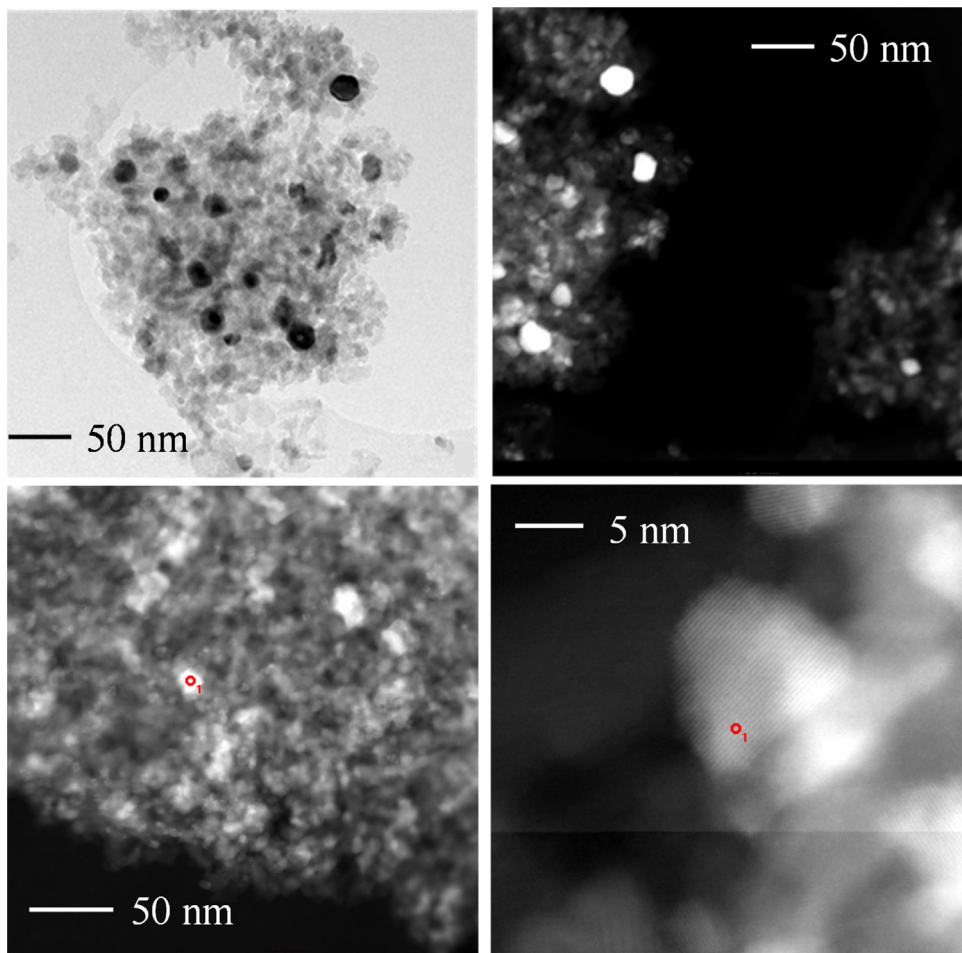


Fig. 2. TEM and Scanning TEM images (Top) of PtPd/CeAl₂O₃ sample, taken after catalytic activity tests and STEM images (Bottom) of PtPd/CeAl₂O₃ sample, taken before activity tests.

both supports partly lost the BET surface area under high temperature pre-treatment of the supports at 900 °C that led to lower particle dispersion during the deposition of the noble metals. EDX analysis of several particles shows the particles contain both Pt and Pd; these results may indicate the formation of alloys between Pt and Pd. Fresh prepared 0.6Pt – 3.2Pd/CeAl₂O₃ sample was also studied by TEM and the images are shown in Fig. 2 (Bottom). A similar alloy formation was noted in this case; however, particle size is smaller than 10 nm.

As described in the Introduction, the active phase of palladium containing catalysts in methane oxidation under lean condition has been suggested to be PdO or Pd-PdO pairs at low temperature and Pd metallic particles at high temperature [4–9]. The re-oxidation ability of Pd-supported catalysts has been widely tested and described in the literature [3,12,16,32]. In the presence of a large amount of oxygen (8 vol.-%), palladium oxidizes into PdO between approx. 300–400 °C and the oxide remains stable in the air (without reductants added) at an atmospheric pressure up to 800 °C. Above this temperature, the stable species are metallic palladium. However, palladium exhibits different reactivity towards oxygen when the temperature is cycled.

In order to correlate the activity of palladium-containing samples synthesized in this study with the formation of PdO species, TPO experiments were performed and the results for the pre-reduced powder samples are shown in Fig. 3. During heating, a negative peak in O₂ signal corresponding to the oxidation of Pd particles to PdO was observed at 359 ± 5 °C for all catalysts tested. For the monometallic Pd catalyst, the peak was sharp, whereas

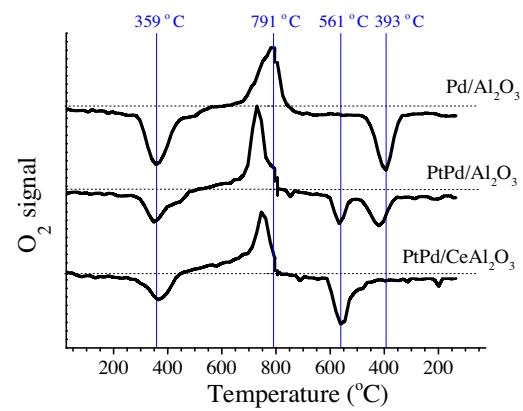


Fig. 3. O₂ evaluation as a function of temperature during ramping up and down for different catalysts. Inlet gas composition: 0.5 vol.-% O₂, Ar; T = RT – 800 °C followed by a decrease to 130 °C; ramp = 10°/min.

for the both Pt-containing samples, the peak was flatter and less intense. The amount of O₂ consumed by the 3.8 wt.-% Pd/Al₂O₃ was 197 μmol/g O₂ per 356 μmol/g palladium, giving O₂/Pd ratio of 0.55, which may be considered as the stoichiometry of the Eq. (1) below.



The behavior of metallic platinum under oxygen excess (8 vol.%) is different from palladium. In oxidizing conditions, PdO forms easily and then decomposes at high temperature (about 800 °C in O₂ excess) where metallic palladium is stable. For platinum, oxide formation is much more difficult; it does occur but requires longer time [33]. It is therefore assumed that the oxygen consumption observed during the heating step in TPO profiles of the bimetallic samples originates mostly from the formation of palladium oxides.

A further increase in temperature resulted in PdO decomposition leading to O₂ release, which can be observed in Fig. 3 by a clear desorption peak. For the monometallic catalyst, a positive peak of O₂ concentration appeared in the TPO profile with a maximum at 791 °C. The peak was broad and associated with the decomposition of different PdO forms, which may coexist on the surface. i.e. PdO in contact with metallic Pd, isolated PdO and PdO strongly interacting with a support, as reported in the literature [16]. The release of O₂ began at lower temperature (730 and 750 °C) for both bimetallic Ce-free and Ce-containing samples, respectively, compared with the oxygen release of the Pd/Al₂O₃ sample. This observation suggests that the PdO decomposition was affected by the presence of Pt. These results are in agreement with the TEM-EDX results, where alloy formation between Pt and Pd was observed. However, the extent of decomposition was not the same for different bimetallic samples.

During the temperature ramp down in the TPO experiments, all three samples demonstrated different behavior. The monometallic sample showed a broad peak with the same amount of O₂ consumed as during heating. However, the O₂ consumption peak occurred at higher temperature during the cooling step (393 °C) compared to heating step (359 °C). The PtPd/Al₂O₃ sample showed two smaller peaks of O₂ consumption at 566 °C and 417 °C. The peak at 566 °C (with a minor shift to lower temperatures) was also observed for the PtPd/CeAl₂O₃ catalyst; however, no peak at 417 °C appeared in that case. For bimetallic samples the loading of Pd was only 301 μmol/g and the O₂ consumption was expected to be 150.5 μmol/g according to the Reaction (1), which is close to the measured values for the reoxidation for both bimetallic samples (138 μmol/g). It should be noted that the oxidation step (when increasing the temperature) consumed less oxygen compared to the re-oxidation for the bi-metallic samples, possibly due to that the bi-metallic samples were not fully reduced during the pre-treatment of the samples before TPO.

It is possible that during the sample preparation both PtPd alloy, as well as Pd particles (or with only a small amount of Pt) were formed for the PtPd/Al₂O₃ sample. This suggestion was confirmed by EDX analysis of fresh PtPd/Al₂O₃ sample (data not shown), however it should be noted that this sample was only degreened in oven in air, which could affect the nano-particle formation. Additionally, high temperature in the presence of oxygen (800 °C) during the TPO may lead to sintering of small Pd particles or altering the alloy formation on the PtPd/Al₂O₃ catalyst which resulted in the formation of less PtPd alloys and more Pd particles. This hypothesis may explain the fact that there are two peaks during re-oxidation of the PtPd/Al₂O₃, whereas only one peak during oxidation. This is also supported by the fact that both Pd/Al₂O₃ and PtPd/Al₂O₃ samples exhibit re-oxidation at low temperature (393 and 417 °C, respectively), which could be attributed to re-oxidation of Pd on Al₂O₃. Interestingly, the ceria-containing sample demonstrated only one re-oxidation peak, compared to the PtPd/Al₂O₃ sample that exhibited two peaks. TEM/EDX measurements of PtPd/CeAl₂O₃ only showed PtPd alloy. Moreover, ceria is a well-known material used to increase the thermal stability of noble metal catalysts [18] and this may then stabilise the PtPd alloy, yielding one type of species that are being reoxidized, which occurs at 561 °C.

The samples were further characterized using CH₄-TPR. Fig. 4 shows the TPR profiles obtained during the catalyst heating from

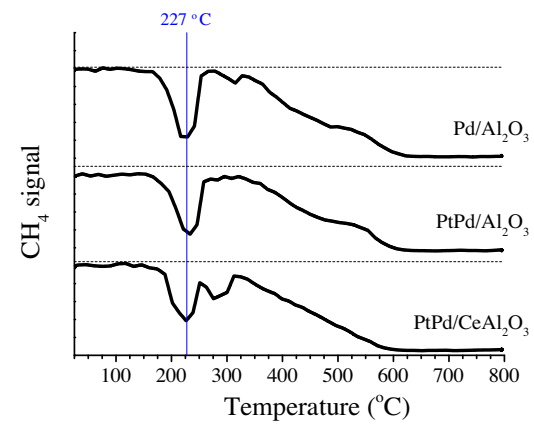
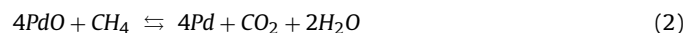


Fig. 4. CH₄-TPR profiles of different catalysts. Inlet gas composition: 0.2 vol.% CH₄, Ar; T = RT – 800 °C; ramp = 10 °C/min.

room temperature to 800 °C. A feature common to all samples was the appearance of a negative peak at 227 °C associated with the CH₄ consumption, with a slight shift observed for the PtPd/Al₂O₃ sample. Based on the TPR data obtained for monometallic sample, the consumption of CH₄ was in agreement with the stoichiometry of the Reaction (2) with ca. 97 μmol/g of CH₄ consumed giving a PdO/CH₄ ratio of 3.7.



The amount of CH₄ consumed was lower for the bimetallic catalysts, which can be attributed to lower Pd loading in comparison with Pd loading of monometallic Pd/Al₂O₃. It should be noted that in the case of the Ce-containing sample, a second peak of CH₄ consumption appeared at 276 °C. However, the total amount of methane consumed was the same as calculated in the case of the bimetallic Ce-free sample. Based on these data, it may be suggested that the PdO interaction with the CeAl₂O₃ support is strong which affects the reducibility of palladium oxide. There was no evidence that the Pt addition promoted any PdO reduction. At a temperature higher than 350 °C, a continuous decrease in CH₄ concentration with increasing temperature was detected. The outlet concentration of CH₄ then reached zero-level at approx. 600 °C.

To understand the consumption of methane during TPR, additional tests on the bimetallic powder samples were performed. Figs. 5 and 6 show the outlet gas flow composition detected during CH₄-TPR and the following oxidation at 800 °C of the bimetallic Ce-free and Ce-containing samples, respectively. As mentioned above, in the case of Ce-free sample, the reduction of PdO occurred with

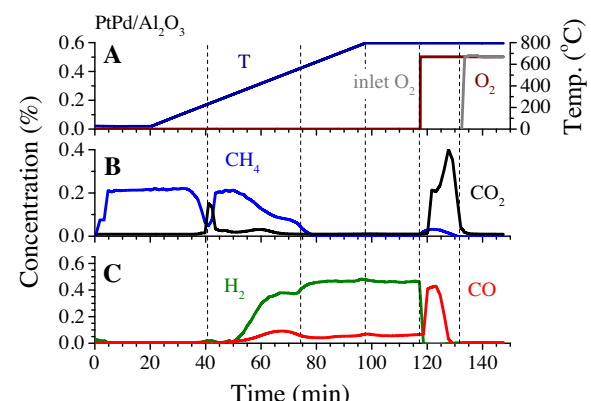


Fig. 5. Outlet gas flow composition monitored during CH₄-TPR over 0.6 wt.% Pt-3.2 wt.% Pd/Al₂O₃. (A) Temperature; inlet and outlet O₂ concentration; (B) concentration of CH₄ and CO₂; (C) concentration of H₂ and CO.

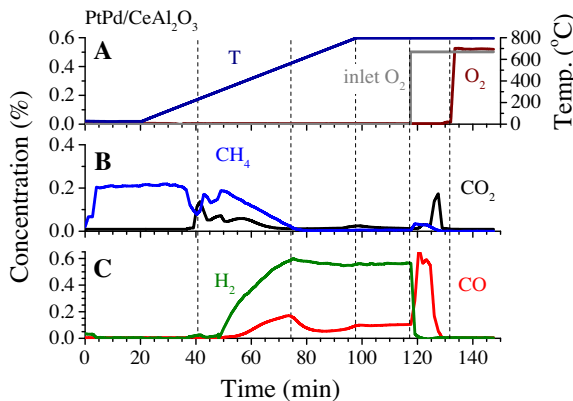


Fig. 6. Outlet gas flow composition monitored during CH₄-TPR over 0.6 wt% Pt-3.2 wt% Pd/CeAl₂O₃. (A) Temperature; inlet and outlet O₂ concentration; (B) concentration of CH₄ and CO₂; (C) concentration of H₂ and CO.

one single peak starting at 200 °C and ending at 260 °C (Fig. 5A). In this case, as can be observed in Fig. 5B, the methane consumption was accompanied by CO₂ formation. A quantitative analysis of the peak area illustrated that methane reacted with PdO, consuming 72 μmol/g CH₄ per 301 μmol/g palladium in the sample, yielding a ratio for PdO/CH₄ of 4.2. This value agrees well with the stoichiometry of the Eq. (2).

In the case of the Ce-containing sample, the reduction was characterized by the presence of two peaks, one centered at 227 °C as shown in Fig. 6A and B, which is the same as for the Ce-free sample, and the other centered at 276 °C. In this case, CO₂ release was also observed. Fig. 6B also shows that the CH₄ concentration decreased with an increase in temperature and that at 600 °C, the conversion of methane reached 100% as described above. During the continuous decrease in CH₄ concentration, no CO₂ formation above 400 °C was detected. However, the signals from H₂ and CO (Fig. 6C) were recorded. If one compares the concentrations of H₂ and CO formed on the Ce-free catalyst (Fig. 5C) with the concentrations obtained on a Ce-containing sample (Fig. 6C), it can be seen that the latter promotes steam reforming (3) and water gas shift (4) Reactions as was reported in the literature [18], which is in line with our results in this study. It was previously reported [34] that a steam reforming Reaction (3) is responsible for methane consumption when palladium oxides are in reduced form.



It should be noted that no H₂O was detected, which probably is due to water storage on the catalyst surface in combination with water consumption during the step (3) and (4). For both samples, in the 312–410 °C temperature region, the main formation of CO₂ was observed (Figs. 5 B and 6 B); however, the amount of CO₂ formed was different. Integration of the consumed and produced species are performed and the results for PtPd/CeAl₂O₃ are shown below. The peak of CO₂ release with a maximum at 383 °C was accompanied by the formation of H₂ and later CO. After the CO₂ concentration decreased, the concentrations of CO and H₂ continuously increased until the maximum values at 550 °C were reached (Fig. 6C). In this temperature region 312–410 °C, methane conversion was not complete. 40 μmol/g of CH₄ was consumed simultaneously as 30 μmol/g of CO; 14 μmol/g of CO₂ and 149 μmol/g of H₂ formed. These values suggest that Reactions (3) and (4) occurred simultaneously and that part of the CO formed in Reaction (3) was consumed in Reaction (4). Between 410 °C and 550 °C the main outlet components formed were CO and H₂ in the 1:4 ratio. In this case, the main reaction was Reaction (3)

accompanied by Reaction (4) to a lesser extent. The data obtained from a quantitative analysis of CH₄ consumed and H₂, CO and CO₂ released during the temperature ramp from 550 °C to 800 °C and the isotherm step at 800 °C for 15 min showed the relation 1:0.4:0.1:2.6 for CH₄:CO:CO₂:H₂, respectively. A large amount of hydrogen was observed during the TPR experiments (Fig. 6C), but less CO and CO₂ were produced than was expected according to the Reactions (3) and (4). An explanation for this is that at high temperature, Reactions (3) and (4) during CH₄-TPR occurred in addition to the formation of coke on the surface of the tested samples by Reaction (5).



Indeed, during the CH₄-TPR step, 740 μmol/g of CH₄ was consumed; however, only 360 μmol/g of CO and CO₂ was released. To confirm possible coke formation, the methane exposure of the catalyst at 800 °C was replaced with O₂, which occurred at approx. 117 min. Fig. 6A shows the outlet and inlet concentrations of O₂. A clear delay in oxygen outlet concentration could be seen. Large CO and then CO₂ formations were observed, with simultaneous O₂ consumption, due to coke oxidation. During this period, the amount of CO and CO₂ formed was 397 μmol/g. Summarising the CO + CO₂ formation during the TPR and oxidation (757 μmol/g), a good agreement is found for the methane consumption (740 μmol/g), resulting in closing the material balance with respect to carbon. It should be noted that the CO/CO₂ ratio was 1:1 for the Ce-free catalyst and 5:1 for the PtPd/CeAl₂O₃ catalyst; thus, a significantly larger amount of CO was produced in the presence of ceria. Moreover, it seems that more coke was formed on the catalysts that does not contain ceria (Fig. 5B and C).

3.2. The effect of water and NO on methane oxidation

The activity of monometallic Pd/Al₂O₃ as well as two bimetallic samples with the same loading of noble metals (approx. 3.8 wt%) was examined during two repetitive temperature ramps, including heating and cooling using water-free and water-containing gas mixtures; the results are displayed in Fig. 7. It should be noted that before water addition the samples were pre-treated at 700 °C and were cooled in Ar flow in order to have a surface free of water species. First, the activity in methane oxidation using merely CH₄ and O₂ was studied (Fig. 7A–C) and the results show that the catalysts were stable when temperature was ramping up and down; and, the activity decreased according to Pd/Al₂O₃ > PtPd/Al₂O₃ > PtPd/CeAl₂O₃, which is in line with the TPO data. For the second cycle higher catalytic activity was obtained during the cooling step for all samples except the one with ceria. Temperature of 50% of methane conversion on Pd/Al₂O₃ during the second temperature ramp down was reached at 283 °C. At this temperature, methane conversion measured on PtPd/Al₂O₃ and PtPd/CeAl₂O₃ was 35% and 25%, respectively. The reason for this could be that the bimetallic samples contain less palladium (3.2 versus 3.8 wt% Pd) and palladium is significantly more active compared to platinum for methane oxidation [11].

Then the activity of the samples was studied in the presence of water vapor in the reaction mixture. As seen in the results presented in Fig. 7D–F, a large deactivation effect was visible when adding 5 vol.% of water. Moreover, the measured activity continuously decreased during the length of the experiment, which can be observed with increasing T₅₀ for the all samples (Table 2). The methane oxidation activity with water is decreased between the two ramps, e.g. T₅₀ for cooling step for Pd/Al₂O₃ sample in the presence of water is increased from 442 °C to 493 °C. The largest temperature increase, was observed for Ce-containing sample from 436 °C to 540 °C. There are several possible reasons for the difference in catalytic activity as discussed in the literature [35]. One

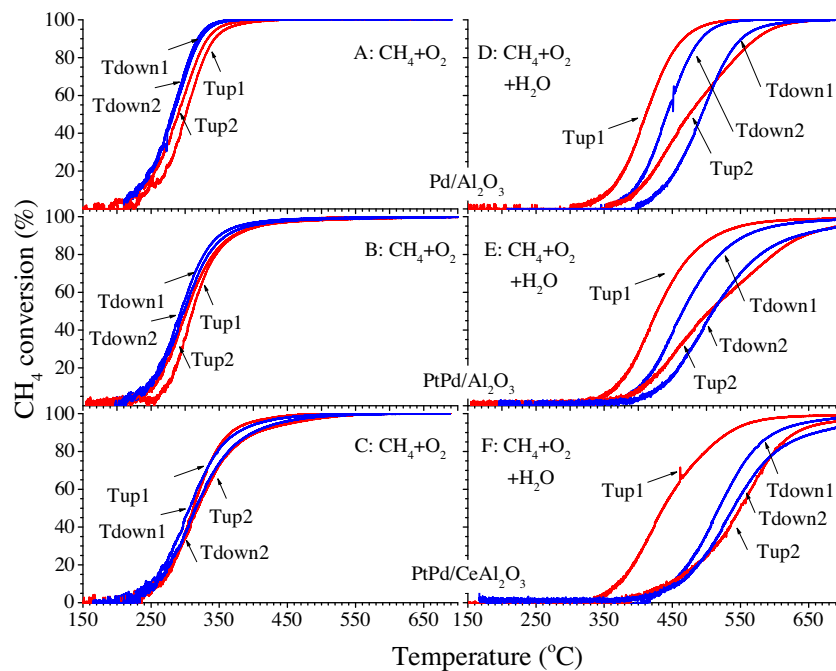


Fig. 7. Methane conversion curves as a function of reaction temperature, obtained over 3 different samples under the ramping up to 700 °C and down to 150 °C repeated twice (ramp rate = 5 °C/min) without pre-treatment between ramps. Inlet gas composition: 0.05 vol.% CH₄, 8 vol.% O₂, Ar (A–C) and 5 vol.% H₂O (added on D–F).

Table 2
Temperature of 50% conversion of CH₄ to CO₂.

Sample	Gas composition	T ₅₀ ramp 1, °C		T ₅₀ ramp 2, °C	
		Heating	Cooling	Heating	Cooling
Pd/Al ₂ O ₃	CH ₄ + O ₂ + H ₂ O	411	442	474	493
	CH ₄ + O ₂ + H ₂ O + NO	420	443	456	482
PtPd/Al ₂ O ₃	CH ₄ + O ₂ + H ₂ O	428	465	505	510
	CH ₄ + O ₂ + H ₂ O + NO	434	462	469	489
PtPd/CeAl ₂ O ₃	CH ₄ + O ₂ + H ₂ O	436	518	549	540
	CH ₄ + O ₂ + H ₂ O + NO	435	503	504	533

possibility is the decomposition of active palladium oxides at high temperature resulting in the formation of less active metallic palladium. However, as was shown by TPO (Fig. 3), all samples exhibited PdO decomposition above 700 °C, which means that PdO decomposition likely did not occur during the activity measurements (Fig. 7). Another possible reason is the formation of different water and hydroxyl species during the ramp up, which block the active sites. It is clear that the second temperature ramp up exhibited significantly lower activity than the first ramp up, even slightly lower activity than the cooling branch in the first ramp. These results demonstrate that the major reason for the lower activity during the cooling branch is likely the formation of hydroxyl species at high temperature during the ramp up experiment. In another study, we developed a kinetic model to propose that there is an immediate deactivation of water, where water or water species likely adsorb fast on the surface, in addition to a second slower deactivation, where hydroxyl species are formed on the active sites (S*), according to the Eq. (6).



We therefore propose that these hydroxyl species are formed during the first temperature ramp up, which results in the less active cooling ramp. Since the process is slow, the second temperature ramp up and down is even less active. Moreover, in the case of 5 vol.% H₂O in the gas mixture, significantly more water was stored on the catalyst surface that was observed during TPD

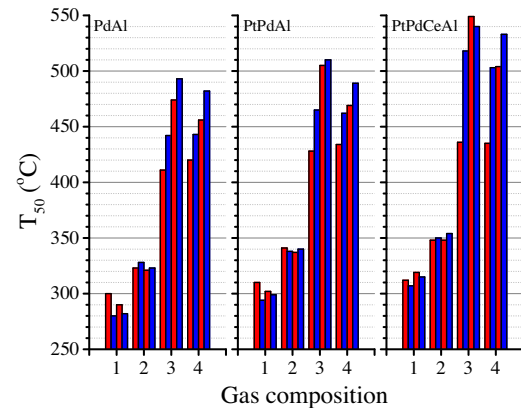


Fig. 8. Comparing the temperature of 50% of methane conversion over 3 different samples under the ramping up to 700 °C and down to 150 °C repeated twice (ramp rate = 5 °C/min) without pre-treatment between ramps. Inlet gas composition: mixture 1: 0.05 vol.% CH₄, 8 vol.% O₂, Ar; mixture 2: mixture 1 + 0.03 vol.% NO; mixture 3: mixture 1 + 5 vol% H₂O; mixture 4: mixture 1 + 0.03 vol.% NO and 5 vol.% H₂O.

experiments (data not shown), which agrees well with the large inhibition of water. Based on the data demonstrated in Fig. 8, comparing the difference between T₅₀ for heating and cooling (Table 2) for each sample, the ceria containing sample exhibits more than twice as large difference than monometallic sample. During the first heating step, the bimetallic samples demonstrated almost the same activity; however, during the next cooling step PtPd/CeAl₂O₃ catalyst was actually less active. These results indicate that more hydroxyl species are formed on the active sites when using the CeAl₂O₃ support.

The effect of NO on dry methane oxidation (without water addition) can be observed in Fig. 8 comparing the T₅₀ obtained for the heating and cooling under different gas compositions. A clear shift of T₅₀ to the high temperature region is seen when comparing the case without water (Fig. 8). It is interesting to note that activity for heating and cooling in the presence of NO were similar between the ramps. We propose that the reason for this is a partial block-

ing of the active sites with NO species, and that this process is rapid and therefore do not cause an increased accumulation on surface with time. Among the three samples, the monometallic sample demonstrated higher activity, e.g. at temperature when monometallic sample had 50% of methane conversion (322°C), the conversion measured on $\text{PtPd}/\text{Al}_2\text{O}_3$ and $\text{PtPd}/\text{CeAl}_2\text{O}_3$ was 33% and 24%, respectively.

The simultaneous presence of H_2O and NO in the gas mixture led to a further decrease in the activity if one compares T_{50} for heating during first temperature ramp (Fig. 8), which could also be explained by the blocking effect of both water and NO. Surprisingly, it is clear that the presence of both water and NO benefits methane oxidation activity during the second temperature ramp up and down which can be clearly seen by comparing the T_{50} in Fig. 8 and Table 2. The presence of NO in the gas flow suppresses the deactivation of the catalyst in methane oxidation by water; an observation that is not widely discussed in the literature. Hurtado et al. [30] found a slightly positive effect on methane oxidation using a $\text{Pd}/\text{Al}_2\text{O}_3$ catalyst when adding 60 ppm NO_2 . In addition, Gremminger et al. [31] observed the reactivation of the $\text{PtPd}/\text{Al}_2\text{O}_3$ catalyst after reaction conditions using NO_x . They speculated that the positive effect was due to the fact that Pt and Pd particles are stabilized in different ways in the presence of NO_x . However, in our experiments, we used also a $\text{Pd}/\text{Al}_2\text{O}_3$ catalyst to ensure that the promoting effect relates to the active palladium sites. A study of $\text{Cu}/\text{ZSM-5}$ by Sjövall et al. [36] may shed some light on NO promoting methane oxidation. In that study, a reaction step was proposed where NO reacted with OH groups to produce HNO_2 species on the surface that were highly active in NH_3 -SCR. Based on this mechanism, it is possible that NO reacts with hydroxyl species to form HNO_2 on the surface also in our study according to the Eq. (7).



Since the hydroxyl species formation was very slow, as discussed above, the formation of HNO_2 will not occur during the first ramp, but instead later when the hydroxyl groups have formed. Indeed, the promotional effect of NO was observed during the heating step of the second ramp, where T_{50} is 18°C lower in the

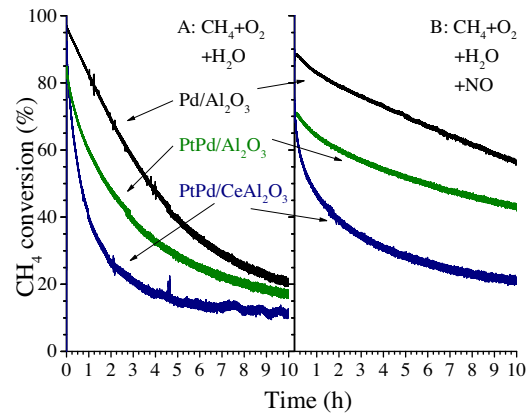


Fig. 9. Catalytic activity in methane oxidation of 3 different samples, measured at constant inlet $T = 450^{\circ}\text{C}$ in 2 different gas mixtures under 10 h. Inlet gas composition: 0.05 vol.% CH_4 , 8 vol.% O_2 , 5 vol.% H_2O , Ar (A) and 0.05 vol.% NO (added on B).

presence of NO for $\text{Pd}/\text{Al}_2\text{O}_3$. For the heating step of the second ramp of bimetallic Ce-free sample, the promotional effect of NO was even greater (36°C). Moreover, similar trends were found for the $\text{PtPd}/\text{CeAl}_2\text{O}_3$ sample, where a clear promotional effect of the addition of NO was observed in the second ramp, where the T_{50} was decreased by as much as 45°C in the presence of NO, showing that this feature can be reproduced on several catalyst formulations.

In order to further study the combined effect of water and NO, isothermal experiments were conducted. In these experiments the samples were first pre-treated at 700°C and cooled in Ar only, to remove water and hydroxyl species from the catalyst surface. The samples were thereafter exposed 500 ppm CH_4 , 8% O_2 and 5% H_2O (see Fig. 9A) or 500 ppm CH_4 , 500 ppm NO, 8% O_2 and 5% H_2O (see Fig. 9B) for 10 h at 450°C . The results in Fig. 9 shows that methane conversion decreased with time and after 10 h of treatment reached 20%, 17% and 12% for $\text{Pd}/\text{Al}_2\text{O}_3$, $\text{PtPd}/\text{Al}_2\text{O}_3$ and $\text{PtPd}/\text{CeAl}_2\text{O}_3$, respectively. When NO was co-fed at 450°C (see Fig. 9b), the decrease in methane conversion was less significant especially for alumina based samples. This type of experiment

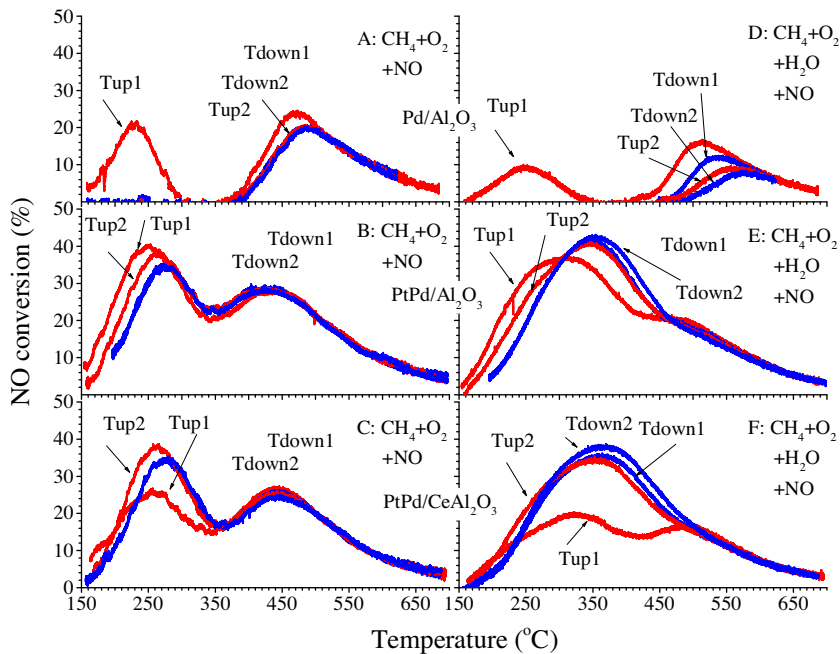


Fig. 10. NO to NO_2 conversion curves as a function of reaction temperature, obtained over 3 different samples under the ramping up to 700°C and down to 150°C repeated twice (ramp rate = $5^{\circ}\text{C}/\text{min}$) without pre-treatment between ramps. Inlet gas composition: 0.05 vol.% CH_4 , 0.05 vol.% NO, 8 vol.% O_2 , Ar (A-C) and 5 vol.% H_2O (added on D-F).

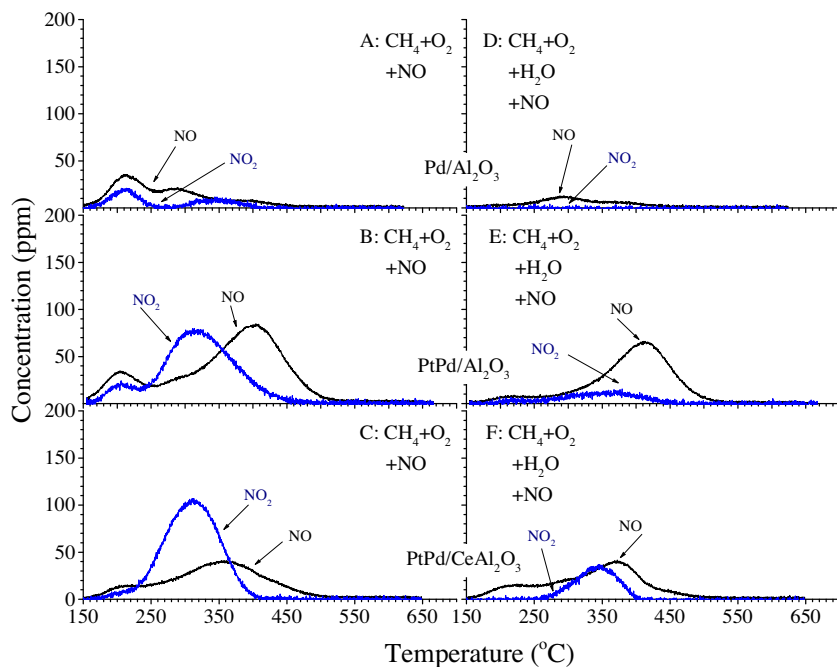


Fig. 11. NO and NO₂ TPD results obtained after catalytic activity tests (Fig. 7) over 3 different samples in Ar flow with a ramp rate of 20°/min. Inlet gas composition for the activity tests: 0.05 vol.% CH₄, 0.05 vol.% NO, 8 vol.% O₂, Ar (A–C) and 5 vol.% H₂O (added on D–F).

clearly shows the promotional effect of NO on water inhibition. Furthermore, it could be seen that samples did not reach the steady-state conditions especially in the case with NO addition, which may relate to that NO delay the deactivation of the catalyst by water.

3.3. NO oxidation and storage during methane oxidation

Oxidation of NO was monitored during methane oxidation experiments mentioned above in relation to Fig. 8. The results in Fig. 10 demonstrate NO to NO₂ conversion under dry (A–C) and wet (D–F) conditions. Monometallic Pd-based sample was less active in NO oxidation, which was expected since it is well known that Pt exhibits high NO oxidation activity. For the Pd/Al₂O₃ sample two NO₂ peaks are observed during the first temperature ramp and the reason for this could be that cooling in Ar only from 700°C resulted in decomposition of the palladium oxides forming metallic Pd. It is possible that the low temperature NO₂ production occurred on the Pd sites. During cooling and also the repeated second ramp the low temperature NO₂ production vanished, and since this occurred both in dry and wet conditions it is likely due to oxidation of the Pd to form PdO, which was not active for low temperature oxidation. Moreover, the NO₂ production was lower for the Pd/Al₂O₃ sample in the presence of water and this could be related to blocking by water and hydroxyl species. Also for the bimetallic samples, in dry gas flow, two clear peaks of NO₂ formation were detected at ca. 270°C and 450°C. Interestingly, these peaks remained during cooling and also in the second ramp, which is different compared to the Pd/Al₂O₃ sample. For the bimetallic samples the main part of the NO oxidation is likely linked to sites in connection to Pt and Pt is likely in metallic form during the cycling, which could explain why the low temperature NO₂ peak is remained. However, Pd/Al₂O₃ samples typically only have one NO₂ peak [37] and we therefore propose that the reason for two peaks is specific properties of the PtPd alloy. Another interesting aspect is that the NO oxidation over the bimetallic samples exhibits one large peak (except for the first heating ramp) in the presence of water. Thus, the water clearly effects the NO oxidation on the PdPt alloy sites.

Fig. 11 illustrates NO and NO₂ data collected during a TPD after the second ramp down in NO oxidation experiments (shown in Fig. 10). There are less NOx stored on the monometallic catalyst, due to the poor NO oxidation activity of Pd. Moreover, it is clearly seen that more NO₂ was stored after the experiments under dry conditions (Fig. 10A–C). From these data it may be suggested that without water more surface nitrates are formed that decompose during TPD with NO₂ release. It is also possible that some of the NO desorbing at high temperature is relating to nitrates that decompose to NO₂ and further dissociate to NO on the Pt sites, due to thermodynamic equilibrium.

4. Conclusions

To conclude, in this study the activity of Pd/Al₂O₃ sample for methane oxidation under lean conditions has been investigated and compared to the activity of PtPd/Al₂O₃ and PtPd/CeAl₂O₃ samples. Without water vapor in the reaction gas mixture, the catalysts showed similar activity after repeating ramping experiments in the temperature interval, 150–700°C. Furthermore, the light-off is often related to the formation of palladium oxides and in order to study the oxidation and decomposition of PdO, TPO experiments were performed. The TPO data showed that the presence of PtPd alloy, which was confirmed with STEM-EDX (Fig. 2), resulted in a decreased temperature for oxide decomposition, as well as an increased temperature for re-oxidation. Moreover, CH₄-TPR experiments were performed in order to study the reduction behavior of the samples.

An inhibition effect of H₂O on methane oxidation over monometallic as well as bimetallic catalysts was illustrated by temperature-programmed experiments, where the second temperature ramp exhibited significantly lower activity compared to the first ramp and we propose that this might be due to the formation of hydroxyl species at high temperatures. These results are consistent with TPD data obtained after the activity tests, showing significantly more water desorption from the experiments with water present during activity tests. Surprisingly, the presence of NO inhibits the CH₄ oxidation under dry conditions likely due to

the blocking effect, but promotes the catalytic activity under wet conditions. An hypothesis for the promotional effect of NO in the presence of water is that hydroxyl species formed at high temperature react with NO to form HNO_2 species on the surface in a similar mechanism as proposed for Cu/ZSM-5 in the literature. Moreover, these species may interact with methane, thereby increasing the methane oxidation activity of the noble-based catalysts. In order to further study this, isothermal experiments were performed at 450 °C. The methane conversion decreased from initial 96% to 25% after 10 h of exposure of the Pd/Al₂O₃ sample in CH₄–O₂–H₂O, while only from 88% to 60% when NO was added to the gas mixture. These results clearly show that the presence of NO enhances the activity. Based on TPD experiments performed after the ramping experiments, less nitrates were present on the surface when water was added to the reaction mixture. Moreover, the NO oxidation was affected by the presence of water, where it was reduced for the Pd/Al₂O₃ sample, but interestingly the observed two NO₂ peaks were combined to one broad peak for the bimetallic samples. The two NO₂ peaks were also observed for the Pd/Al₂O₃ sample in both dry and wet conditions, however, the low temperature peak vanished after the first temperature ramping experiment. The reason could be that metallic Pd sites were present after the pre-treatment which might result in the low temperature activity.

Acknowledgments

The project is a collaboration between AVL MTC Motortestcenter AB, Johnson Matthey AB, Scania CV AB and the Chalmers University of Technology. The Swedish Energy Agency (FFI 37179-1) is gratefully acknowledged for its financial support.

References

- [1] H. Engerer, M. Horn, Natural gas vehicles: an option for Europe, *Energy Policy* 38 (2010) 1017–1029, <http://dx.doi.org/10.1016/j.enpol.2009.10.054>.
- [2] P. Gélin, M. Primet, Complete oxidation of methane at low temperature over noble metal based catalysts: a review, *Appl. Catal. B: Environ.* 39 (2002) 1–37, [http://dx.doi.org/10.1016/S0926-3373\(02\)00076-0](http://dx.doi.org/10.1016/S0926-3373(02)00076-0).
- [3] D. Ciuparu, M.R. Lyubovsky, E. Altman, L.D. Pfefferle, A. Datye, Catalytic combustion of methane over palladium –based catalysts, *Catal. Rev.* 44 (2002) 593–649, <http://dx.doi.org/10.1081/CR-120015482>.
- [4] J. Nilsson, P.-A. Carlsson, S. Fouladvand, N.M. Martin, J. Gustafson, M.A. Newton, E. Lundgren, H. Grönbeck, M. Skoglundh, Chemistry of supported palladium nanoparticles during methane oxidation, *ACS Catal.* 5 (2015) 2481–2489, <http://dx.doi.org/10.1021/cs502036d>.
- [5] N.M. Kinnunen, J.T. Hirvi, T. Venäläinen, M. Suvanto, T.A. Pakkanen, Procedure to tailor activity of methane combustion catalyst: relation between Pd/PdO_x active sites and methane oxidation activity, *Appl. Catal. Gen.* 397 (2011) 54–61, <http://dx.doi.org/10.1016/j.apcata.2011.02.013>.
- [6] D. Gao, C. Zhang, S. Wang, Z. Yuan, S. Wang, Catalytic activity of Pd/Al₂O₃ toward the combustion of methane, *Catal. Commun.* 9 (2008) 2583–2587, <http://dx.doi.org/10.1016/j.catcom.2008.07.014>.
- [7] S. Colussi, A. Trovarelli, G. Groppi, J. Llorca, The effect of CeO₂ on the dynamics of Pd–PdO transformation over Pd/Al₂O₃ combustion catalysts, *Catal. Commun.* 8 (2007) 1263–1266, <http://dx.doi.org/10.1016/j.catcom.2006.11.020>.
- [8] A.K. Datye, J. Bravo, T.R. Nelson, P. Atanasova, M. Lyubovsky, L. Pfefferle, Catalyst microstructure and methane oxidation reactivity during the Pd \leftrightarrow PdO transformation on alumina supports, *Appl. Catal. Gen.* 198 (2000) 179–196, [http://dx.doi.org/10.1016/S0926-860X\(99\)00512-8](http://dx.doi.org/10.1016/S0926-860X(99)00512-8).
- [9] K. Fujimoto, F.H. Ribeiro, M. Avalos-Borja, E. Iglesia, Structure and reactivity of PdO_x/ZrO₂ catalysts for methane oxidation at low temperatures, *J. Catal.* 179 (1998) 431–442, <http://dx.doi.org/10.1006/jcat.1998.2178>.
- [10] M. Lyubovsky, L.L. Smith, M. Castaldi, H. Karim, B. Nentwick, S. Etemad, R. LaPierre, W.C. Pfefferle, Catalytic combustion over platinum group catalysts: fuel-lean versus fuel-rich operation, *Catal. Today* 83 (2003) 71–84, [http://dx.doi.org/10.1016/S0920-5861\(03\)00217-7](http://dx.doi.org/10.1016/S0920-5861(03)00217-7).
- [11] R. Burch, P.K. Loader, Investigation of Pd/Al₂O₃ and Pd/Al₂O₃ catalysts for the combustion of methane at low concentrations, *Appl. Catal. B: Environ.* 5 (1994) 149–164, [http://dx.doi.org/10.1016/0926-3373\(94\)00037-9](http://dx.doi.org/10.1016/0926-3373(94)00037-9).
- [12] K. Persson, K. Jansson, S. Järås, Characterisation and microstructure of Pd and bimetallic Pd–Pt catalysts during methane oxidation, *J. Catal.* 245 (2007) 401–414, <http://dx.doi.org/10.1016/j.jcat.2006.10.029>.
- [13] N.M. Kinnunen, J.T. Hirvi, M. Suvanto, T.A. Pakkanen, Methane combustion activity of Pd–PdO_x–Pt/Al₂O₃ catalyst: the role of platinum promoter, *J. Mol. Catal. Chem.* 356 (2012) 20–28, <http://dx.doi.org/10.1016/j.molcata.2011.12.023>.
- [14] K. Narui, H. Yata, K. Furuta, A. Nishida, Y. Kohtoku, T. Matsuzaki, Effects of addition of Pt to PdO/Al₂O₃ catalyst on catalytic activity for methane combustion and TEM observations of supported particles, *Appl. Catal. Gen.* 179 (1999) 165–173, [http://dx.doi.org/10.1016/S0926-860X\(98\)00306-8](http://dx.doi.org/10.1016/S0926-860X(98)00306-8).
- [15] H. Yamamoto, H. Uchida, Oxidation of methane over Pt and Pd supported on alumina in lean-burn natural-gas engine exhaust, *Catal. Today* 45 (1998) 147–151, [http://dx.doi.org/10.1016/S0920-5861\(98\)00265-X](http://dx.doi.org/10.1016/S0920-5861(98)00265-X).
- [16] P. Castellazzi, G. Groppi, P. Forzatti, Effect of Pt/Pd ratio on catalytic activity and redox behavior of bimetallic Pt–Pd/Al₂O₃ catalysts for CH₄ combustion, *Appl. Catal. B: Environ.* 95 (2010) 303–311, <http://dx.doi.org/10.1016/j.apcatb.2010.01.008>.
- [17] X. Fan, F. Wang, T. Zhu, H. He, Effects of Ce on catalytic combustion of methane over Pd–Pt/Al₂O₃ catalyst, *J. Environ. Sci.* 24 (2012) 507–511, [http://dx.doi.org/10.1016/S1001-0742\(11\)60798-5](http://dx.doi.org/10.1016/S1001-0742(11)60798-5).
- [18] A. Trovarelli, Catalytic properties of ceria and CeO₂-containing materials, *Catal. Rev.* 38 (1996) 439–520, <http://dx.doi.org/10.1080/01614949608006464>.
- [19] S. Colussi, A. Trovarelli, E. Vesselli, A. Baraldi, G. Comelli, G. Groppi, J. Llorca, Structure and morphology of Pd/Al₂O₃ and Pd/CeO₂/Al₂O₃ combustion catalysts in Pd–PdO transformation hysteresis, *Appl. Catal. Gen.* 390 (2010) 1–10, <http://dx.doi.org/10.1016/j.apcata.2010.09.033>.
- [20] R. Ramírez-López, I. Elizalde-Martínez, L. Balderas-Tapia, Complete catalytic oxidation of methane over Pd/CeO₂–Al₂O₃: the influence of different ceria loading, *Catal. Today* 150 (2010) 358–362, <http://dx.doi.org/10.1016/j.cattod.2009.10.007>.
- [21] P. Hurtado, Development of a kinetic model for the oxidation of methane over Pd/Al₂O₃ at dry and wet conditions, *Appl. Catal. B: Environ.* 51 (2004) 229–238, <http://dx.doi.org/10.1016/j.apcatb.2004.03.006>.
- [22] V. Dupont, J.M. Jones, S.-H. Zhang, A. Westwood, M.V. Twigg, Kinetics of methane oxidation on Pt catalysts in the presence of H₂S and SO₂, *Chem. Eng. Sci.* 59 (2004) 17–29, <http://dx.doi.org/10.1016/j.ces.2003.08.023>.
- [23] R. Burch, F. Urbano, P. Loader, Methane combustion over palladium catalysts: the effect of carbon dioxide and water on activity, *Appl. Catal. Gen.* 123 (1995) 173–184, [http://dx.doi.org/10.1016/0926-860X\(94\)00251-7](http://dx.doi.org/10.1016/0926-860X(94)00251-7).
- [24] G. Zhu, J. Han, D.Y. Zemlyanov, F.H. Ribeiro, Temperature dependence of the kinetics for the complete oxidation of methane on palladium and palladium oxide, *J. Phys. Chem. B* 109 (2005) 2331–2337, <http://dx.doi.org/10.1021/jp0488665>.
- [25] F.H. Ribeiro, M. Chow, R.A. Dallabetta, Kinetics of the complete oxidation of methane over supported palladium catalysts, *J. Catal.* 146 (1994) 537–544, <http://dx.doi.org/10.1006/jcat.1994.1092>.
- [26] R. Abbasi, L. Wu, S.E. Wanke, R.E. Hayes, Kinetics of methane combustion over Pt and Pt–Pd catalysts, *Chem. Eng. Res. Des.* 90 (2012) 1930–1942, <http://dx.doi.org/10.1016/j.cherd.2012.03.003>.
- [27] R. Monteiro, D. Zemlyanov, J. Storey, F. Ribeiro, Turnover rate and reaction orders for the complete oxidation of methane on a palladium foil in excess dioxygen, *J. Catal.* 199 (2001) 291–301, <http://dx.doi.org/10.1006/jcat.2001.3176>.
- [28] G. Groppi, W. Ihashi, M. Valentini, P. Forzatti, High-temperature combustion of CH₄ over PdO/Al₂O₃: kinetic measurements in a structured annular reactor, *Chem. Eng. Sci.* 56 (2001) 831–839, [http://dx.doi.org/10.1016/S0009-2509\(00\)00295-5](http://dx.doi.org/10.1016/S0009-2509(00)00295-5).
- [29] W.R. Schwartz, L.D. Pfefferle, Combustion of methane over palladium-based catalysts: support interactions, *J. Phys. Chem. C* 116 (2012) 8571–8578, <http://dx.doi.org/10.1021/jp2119668>.
- [30] P. Hurtado, S. Ordóñez, H. Sastre, F. Díez, Combustion of methane over palladium catalyst in the presence of inorganic compounds: inhibition and deactivation phenomena, *Appl. Catal. B: Environ.* 47 (2004) 85–93, [http://dx.doi.org/10.1016/S0926-3373\(03\)00328-X](http://dx.doi.org/10.1016/S0926-3373(03)00328-X).
- [31] A.T. Gremminger, H.W. Pereira de Carvalho, R. Popescu, J.-D. Grunwaldt, O. Deutschmann, Influence of gas composition on activity and durability of bimetallic Pt–Pd/Al₂O₃ catalysts for total oxidation of methane, *Catal. Today* 258 (2015), <http://dx.doi.org/10.1016/j.cattod.2015.01.034>.
- [32] K. Persson, A. Ersson, K. Jansson, J. Fierro, S. Järås, Influence of molar ratio on Pd–Pt catalysts for methane combustion, *J. Catal.* 243 (2006) 14–24, <http://dx.doi.org/10.1016/j.jcat.2006.06.019>.
- [33] L. Olsson, E. Fridell, The influence of Pt oxide formation and Pt dispersion on the reactions $\text{NO}_2 \leftrightarrow \text{NO} + 1/2 \text{O}_2$ over Pt/Al₂O₃ and Pt/BaO/Al₂O₃, *J. Catal.* 210 (2002) 340–353, <http://dx.doi.org/10.1006/jcat.2002.3698>.
- [34] P. Castellazzi, G. Groppi, P. Forzatti, A. Baylet, P. Marécot, D. Duprez, Role of Pt loading and dispersion on redox behaviour and CH₄ combustion activity of Al₂O₃ supported catalysts, *Catal. Today* 155 (2010) 18–26, <http://dx.doi.org/10.1016/j.cattod.2009.02.029>.
- [35] A. Amin, A. Abedi, R. Hayes, M. Votsmeier, W. Epling, Methane oxidation hysteresis over Pt/Al₂O₃, *Appl. Catal. Gen.* 478 (2014) 91–97, <http://dx.doi.org/10.1016/j.apcata.2014.03.032>.
- [36] H. Sjövall, R.J. Blint, L. Olsson, Detailed kinetic modeling of NH₃ SCR over Cu-ZSM-5, *Appl. Catal. B: Environ.* 92 (2009) 138–153, <http://dx.doi.org/10.1016/j.apcatb.2009.07.020>.
- [37] X. Auvray, L. Olsson, Stability and activity of Pd–Pt–Pd catalysts supported on alumina for NO oxidation, *Appl. Catal. B: Environ.* 168–169 (2015) 342–352, <http://dx.doi.org/10.1016/j.apcatb.2014.12.035>.